



# Impact of deep learning-based reconstruction and anti-peristaltic agent on the image quality and diagnostic performance of magnetic resonance enterography comparing single breath-hold single-shot fast spin echo with and without anti-peristaltic agent

Eun Joo Park<sup>1</sup>, Yedaun Lee<sup>1</sup>, Ho-Joon Lee<sup>1</sup>, Jung Hee Son<sup>1</sup>, Jisook Yi<sup>1</sup>, Seok Hahn<sup>1</sup>, Joonsung Lee<sup>2</sup>

<sup>1</sup>Department of Radiology, Inje University College of Medicine, Haeundae Paik Hospital, Busan, Republic of Korea; <sup>2</sup>GE HealthCare Korea, Seoul, Republic of Korea

**Contributions:** (I) Conception and design: Y Lee, HJ Lee; (II) Administrative support: Y Lee; (III) Provision of study materials or patients: EJ Park, Y Lee; (IV) Collection and assembly of data: EJ Park, JH Son, J Yi, S Hahn; (V) Data analysis and interpretation: EJ Park, Y Lee, HJ Lee, J Lee; (VI) Manuscript writing: All authors; (VII) Final approval of manuscript: All authors.

**Correspondence to:** Yedaun Lee, MD, PhD. Department of Radiology, Inje University College of Medicine, Haeundae Paik Hospital, 875 Haeundae-ro, Haeundae-gu, Busan, Republic of Korea. Email: chosai81@gmail.com.

**Background:** While anti-peristaltic agents are beneficial for high quality magnetic resonance enterography (MRE), their use is constrained by potential side effects and increased examination complexity. We explored the potential of deep learning-based reconstruction (DLR) to compensate for the absence of anti-peristaltic agent, improve image quality and reduce artifact. This study aimed to evaluate the need for an anti-peristaltic agent in single breath-hold single-shot fast spin-echo (SSFSE) MRE and compare the image quality and artifacts between conventional reconstruction (CR) and DLR.

**Methods:** We included 45 patients who underwent MRE for Crohn's disease between October 2021 and September 2022. Coronal SSFSE images without fat saturation were acquired before and after anti-peristaltic agent administration. Four sets of data were generated: SSFSE CR with and without an anti-peristaltic agent (CR-A and CR-NA, respectively) and SSFSE DLR with and without an anti-peristaltic agent (DLR-A and DLR-NA, respectively). Two radiologists independently reviewed the images for overall quality and artifacts, and compared the three images with DLR-A. The degree of distension and inflammatory parameters were scored on a 5-point scale in the jejunum and ileum, respectively. Signal-to-noise ratio (SNR) levels were calculated in superior mesenteric artery (SMA) and iliac bifurcation level.

**Results:** In terms of overall quality, DLR-NA demonstrated no significant difference compared to DLR-A, whereas CR-NA and CR-A demonstrated significant differences ( $P < 0.05$ , both readers). Regarding overall artifacts, reader 1 rated DLR-A slightly better than DLR-NA in four cases and rated them as identical in 41 cases ( $P = 0.046$ ), whereas reader 2 demonstrated no difference. Bowel distension was significantly different in the jejunum (Reader 1:  $P = 0.046$ ; Reader 2:  $P = 0.008$ ) but not in the ileum. Agreements between the images (Reader 1:  $\kappa = 0.73$ – $1.00$ ; Reader 2:  $\kappa = 1.00$ ) and readers ( $\kappa = 0.66$  for all comparisons) on inflammation were considered good to excellent. The sensitivity, specificity, and accuracy in diagnosing inflammation in the terminal ileum were the same among DLR-NA, DLR-A, CR-NA and CR-A (94.42%, 81.83%, and 89.69%; and 83.33%, 90.91%, and 86.21% for Readers 1 and 2, respectively). In both SMA and iliac bifurcation levels, SNR of DLR images exhibited no significant differences. CR images showed significantly lower SNR compared with DLR images ( $P < 0.001$ ).

**Conclusions:** SSFSE without anti-peristaltic agents demonstrated nearly equivalent quality to that with anti-peristaltic agents. Omitting anti-peristaltic agents before SSFSE and adding DLR could improve the scanning outcomes and reduce time.

**Keywords:** Magnetic resonance enterography (MRE); anti-peristaltic agents; deep learning-based reconstruction (DLR)

Submitted May 29, 2023. Accepted for publication Oct 25, 2023. Published online Jan 02, 2024.

doi: 10.21037/qims-23-738

View this article at: <https://dx.doi.org/10.21037/qims-23-738>

## Introduction

For high-quality magnetic resonance enterography (MRE), adequate bowel distension and the absence of bowel movement are essential (1). Anti-peristaltic agents are widely used to decrease bowel peristalsis and improve bowel distension, subsequently reducing image blurring, which could degrade image quality. Although a previous study reported that diagnostic confidence remains high without using an anti-peristaltic agent (2), its administration is considered beneficial for enhancing image quality, and as a result, current international guidelines suggest considering its application (3,4).

Although the time and dose of administration vary among institutions, split-dose administration is considered more effective than single-dose administration for reducing peristalsis (5). Current guidelines recommend split-dose administration for improving image quality, and many institutions follow this recommendation (6,7). T1-weighted three-dimensional (3D) spoiled gradient-echo sequences are most susceptible to bowel movement; therefore, injection of anti-peristaltic agents before T1-weighted imaging (T1WI) is a common practice (1). Moreover, a previous study demonstrated that omitting anti-peristaltic agent administration could decrease the sensitivity of diffusion-weighted imaging (DWI) for diagnosing bowel inflammation in Crohn's disease (8). Thus, anti-peristaltic agents are administered before T2WI, DWI, and T1WI at our institution.

Despite the benefits of anti-peristaltic agents, their use could be limited owing to the side effects attributed to their anticholinergic properties, and increased complexity and expense of the examination. Therefore, reducing the use of anti-peristaltic agents, while preserving the diagnostic performance could make MRE examinations more convenient, less costly, and less likely to result in adverse effects.

Single-shot fast spin-echo (SSFSE), which obtains images within a single echo train, is routinely used for T2-weighted MRE. SSFSE can be performed very quickly within single breath-hold, making it less susceptible to bowel movements than other sequences (9). Moreover, omitting the use of

anti-peristaltic agents before performing SSFSE could be considered feasible. However, the possibility of image degradation owing to image blurring may affect diagnostic capability.

Recently, a deep learning-based reconstruction (DLR) pipeline (AIR Recon DL, GE Healthcare, Waukesha, USA) was used to provide high-quality images with reduced image blurring. The DLR pipeline utilizes raw k-space data as input and produces high-quality images as output, simultaneously with the MRI acquisition (10). Previous reports have demonstrated that DLR can improve image quality and reduce artifacts in T2-weighted abdominal imaging (11,12). Our hypothesis stated that DLR could compensate for image degradation attributed to the absence of an anti-peristaltic agent and provide higher-quality images compared to SSFSE with conventional reconstruction. Thus, we compared the image quality of single breath-hold SSFSE using conventional reconstruction and single breath-hold SSFSE using DLR with and without an anti-peristaltic agent and evaluated their diagnostic performance for active inflammation in Crohn's disease.

## Methods

This study was approved by the institutional review board of Inje University Haeundae Paik Hospital (No. HPIRB 2023-04-016-002). The requirement for informed consent was waived owing to the retrospective nature of the study. The study was conducted in accordance with the Declaration of Helsinki (as revised in 2013).

### *Patients*

This retrospective study included 45 patients (31 men, 14 women; mean age, 31.5±9.5 years) who underwent MRE for known Crohn's disease between October 2021 and September 2022.

### *Image acquisition*

MRE was performed using a 3T MR imaging (MRI)

scanner (SIGNA™ Architect, GE Healthcare, Waukesha, USA) with two 30-channel coils (AIR™ anterior array coil, GE Healthcare, Waukesha, USA).

Prior to image acquisition, the patients ingested 1,000 mL of polyethylene glycol solution (Coolprep, Taejoon Pharm, Seoul, South Korea) to ensure adequate bowel distension. A total of 7.5 mg cimetropium bromide (Alpit, Hana Pharmaceutical Co., Seoul, Korea) was administered in three divided doses during the examination; the first dose was administered just before the second scan of the T2-weighted coronal image, the second dose was administered just before DWI, and the third dose was administered just before obtaining the coronal T1-weighted images.

Coronal SSFSE T2-weighted images without fat saturation were acquired within single breath-hold before and after anti-peristaltic agent administration, followed by image reconstruction using conventional reconstruction (CR) and DLR methods. The following four sets of data were generated: CR SSFSE with an antiperistaltic agent (CR-A), DLR SSFSE with an antiperistaltic agent (DLR-A), CR SSFSE without an antiperistaltic agent (CR-NA), and DLR SSFSE without an antiperistaltic agent (DLR-NA). The detailed imaging parameters are listed in [Table S1](#).

### **DLR**

Commercially available DLR pipeline (AIR™ Recon DL, GE Healthcare, Waukesha, USA) based on deep convolutional neural network (CNN). The DLR pipeline takes raw k-space data as its input and generates high fidelity images as its output. The CNN contains 4.4 million trainable parameters in approximately 10,000 kernels (10). The network was trained using pairs of images representing near perfect and conventional MRI images. DLR reduces truncation artifacts, increases sharpness, and offers tunable noise reduction levels. A reduction factor of 75% (DL High) was selected for this study. Our decision to apply the 75% (DL High) was substantiated through a comprehensive evaluation of noise reduction options, including 25% (DL Low) and 50% (DL Medium) levels, wherein we came to consensus that the 75% (DL High) was the most optimal for improving the image quality (10,13).

### **Image analysis**

Two board-certified radiologists (with 2 and 12 years of abdominal radiology experience, respectively) who were blinded to the clinical information, except for the diagnosis

of Crohn's disease, independently reviewed the images. Two readers reviewed CR-A, DLR-NA, and CR-NA with a side-by-side comparison, using DLR-A as a reference standard. The readers evaluated the overall image quality and artifacts using the following 5-point scale: 1 = DLR-A is much better, 2 = DLR-A is slightly better, 3 = identical quality as DLR-A, 4 = slightly better quality than DLR-A, and much better quality than DLR-A (14,15). Both overall image quality and overall artifacts were subjectively assessed. In the evaluation of overall image quality, readers considered the image's suitability for lesion detection, taking into account factors such as noise, artifacts, sharpness, and contrast. When assessing overall artifacts, readers examined the presence and extent of various issues, including motion artifacts caused by bowel peristalsis, ghosting artifacts, and FID artifacts.

Since reconstruction methods provide no benefit for bowel distension, the bowel distension degree was only evaluated using DLR-A and DLR-NA images. The extent of bowel distension was evaluated using the following grading scale: 1 = all bowel loops are collapsed without luminal separation, and the walls cannot be recognized; 2 = adequate bowel distension is visible in less than 50%; 3 = adequate bowel distension is visible in 50–80% of the segments; 4 = more than 80% of bowel loops are adequately distended; and 5 = all bowel loops in the segment are adequately distended. Adequate bowel distension was defined as bowel diameter more than 1.5 cm (16). For consistent interpretation, jejunal loops were defined as small bowel loops located on the upper and left sides of the abdominal wall, with thicker plicae circulares and densely arranged folds. The ileal loops were characterized by thinner circular plicae with loose arrangement, mainly in the lower compartment of the abdomen (16).

The parameters of active inflammation were assessed based on the bowel wall thickness, and mural and perimural signal intensity in the jejunum and ileum, respectively using a 4-point scale (17). This evaluation was conducted using only T2-weighted images. The detailed scoring system is presented in [Table 1](#).

Each reader evaluated the sensitivity, specificity, and accuracy of the diagnosis of ileal and jejunal inflammation. Only the terminal ileum was selected to avoid overestimation of the diagnostic performance owing to multifocal involvement of the ileum. The reference standard for terminal ileal inflammation was determined by the endoscopic results obtained within one week prior to or following the MRE examination. For the jejunum, an

**Table 1** The scoring system of bowel inflammation

Parameter	Scoring			
	0	1	2	3
Bowel wall thickness (mm)	1–3	>3–5	>5–7	>7
Mural signal intensity on T2 weighted image	Equivalent to that of normal bowel wall	Minor increase in signal intensity	Moderate increase in signal intensity	Marked increase in signal intensity; bowel wall contains areas of high signal intensity, approaching that of the luminal content
Perimural signal intensity on T2 weighted images	Equivalent to that of normal mesentery	Increase in mesenteric signal intensity but no fluid collection	Small fluid rim ( $\leq 2$ mm)	Large fluid rim ( $> 2$ mm)

abdominal radiologist reviewed all the available sequences to determine the presence of active inflammation in the jejunal loops, which were used as the reference standard.

The signal-to-noise ratio (SNR) was calculated in two slices, at the level of superior mesenteric artery (SMA) and iliac bifurcation of aorta. The mean signal of the image slice was calculated, and it was divided by estimated standard deviation of noise level. The noise level was estimated by a hybrid discrete wavelet transform (DWT) and edge information removal-based algorithm (18,19).

### Statistical analysis

The scores for the overall image quality, artifacts, and bowel distension were compared using a paired-sample Wilcoxon signed-rank test. The inter-reader and inter-sequence agreement of bowel wall thickness, mural signal intensity, and perimural signal intensity were calculated using Cohen's kappa coefficients ( $\kappa$ ). The kappa value was interpreted as poor, fair, moderate, good, and excellent agreement for  $\kappa < 0.2$ , 0.21–0.4, 0.41–0.60, 0.61–0.80, and 0.81–1.0, respectively. The SNR between four images were compared using the Friedman test. Statistical significance was set at  $P < 0.05$ . The Bonferroni correction was used for multiple comparison in the SNR comparison. Statistical analyses were performed using SPSS Statistics for Windows, version 28.0 (IBM Corp., Armonk, NY, USA).

## Results

### Comparison of the qualitative scores

In terms of overall quality, DLR-NA demonstrated no significant difference in the scores compared with DLR-A (Reader 1:  $P = 0.157$ ; Reader 2:  $P = 0.317$ ). CR-NA and

CR-A demonstrated significant differences compared to DLR-A (both readers,  $P < 0.05$ ). DLR-NA and DLR-A were mostly equivalent in terms of image quality for both readers (43 and 44 cases for Readers 1 and 2, respectively). However, when compared to CR-NA and CR-A, DLR-A demonstrated slightly better image quality in more cases (12 cases for CR-NA and eight cases for CR-A by Reader 1; 39 cases for CR-NA and 39 cases for CR-A by Reader 2).

Considering the overall artifacts, no significant difference was observed between DLR-NA and DLR-A for Reader 2 ( $P = 0.317$ ). Reader 1 found that DLR-A was slightly better than DLR-NA in four cases and identical in 41 cases ( $P = 0.046$ ). CR-NA and CR-A demonstrated significant differences in the overall artifacts when compared with DLR-A, with majority of the DLR-A images graded showing slightly better quality than the CR-NA or CR-A images ( $P < 0.001$ ). The detailed results are summarized in *Table 2*.

Both readers found a statistically significant difference in the bowel distension score between DLR-A and DLR-NA in the jejunum [Reader 1: DLR-NA,  $2.78 \pm 0.70$  (mean  $\pm$  standard deviation); DLR-A,  $2.87 \pm 0.79$ ;  $P = 0.046$ ; and Reader 2: DLR-NA,  $2.73 \pm 0.72$ ; DLR-A,  $2.89 \pm 0.71$ ;  $P = 0.008$ ], whereas no significant difference was observed in the ileal loop by either reader (Reader 1: DLR-NA,  $3.44 \pm 0.59$ ; DLR-A,  $3.51 \pm 0.59$ ;  $P = 0.083$ ; and Reader 2: DLR-NA,  $3.98 \pm 0.66$ ; DLR-A,  $4.00 \pm 0.67$ ;  $P = 0.317$ ). The results are presented in *Table 3*.

### Comparison of the inflammatory parameters

The inter-image agreement of the parameters of active inflammation in both readers demonstrated moderate to excellent agreement (Reader 1:  $\kappa = 0.49$ –1.00; Reader 2:  $\kappa$

**Table 2** Comparison of the qualitative scores of image quality and artifacts in the four images.

Measures	Images	Scoring scales	Number of patients	
			Reader 1	Reader 2
Overall image quality	DLR-NA	DLR-A slightly better than DLR-NA	2	1
		DLR-NA and DLR-A identical	43	44
		DLR-NA slightly better than DLR-A	0	0
		P value	0.157	0.317
	CR-NA	DLR-A slightly better than CR-NA	12	39
		CR-NA and DLR-A identical	33	6
		CR-NA slightly better than DLR-A	0	0
		P value	0.001	<0.001
	CR-A	DLR-A slightly better than CR-A	8	39
		CR-A and DLR-A identical	37	6
		CR-A slightly better than DLR-A	0	0
		P value	0.005	<0.001
Overall artifact	DLR-NA	DLR-A slightly better than DLR-NA	4	1
		DLR-NA and DLR-A identical	41	44
		DLR-NA slightly better than DLR-A	0	0
		P value	0.046	0.317
	CR-NA	DLR-A slightly better than CR-NA	35	39
		CR-NA and DLR-A identical	10	6
		CR-NA slightly better than DLR-A	0	0
		P value	<0.001	<0.001
	CR-A	DLR-A slightly better than CR-A	34	39
		CR-A and DLR-A identical	11	6
		CR-A slightly better than DLR-A	0	0
		P value	<0.001	<0.001

No scores were given for any qualitative measure of image quality, indicating that the DLR-A image was significantly better than the other images (DLR-NA, CR-NA, and CR-A) or that any of these other images were significantly better than DLR-A. DLR-NA, SSFSE with deep learning-based reconstruction without anti-peristaltic agent; CR-NA, SSFSE with conventional reconstruction without anti-peristaltic agent; CR-A, SSFSE with conventional reconstruction with anti-peristaltic agent; DLR-A, SSFSE with deep learning-based reconstruction with an anti-peristaltic agent; SSFSE, single-shot fast spin-echo.

**Table 3** Comparison of bowel distension scores based on presence of anti-peristalsis agent

Bowel segment	Reader 1			Reader 2		
	DLR-NA	DLR-A	P value	DLR-NA	DLR-A	P value
Jejunum	2.78±0.70	2.87±0.79	0.046	2.73±0.72	2.89±0.71	0.008
Ileum	3.44±0.59	3.51±0.59	0.083	3.98±0.66	4.00±0.67	0.317

Values are presented as mean ± standard deviation. DLR-NA, SSFSE with deep learning-based reconstruction without anti-peristaltic agent; DLR-A, SSFSE with deep learning-based reconstruction with an anti-peristaltic agent; SSFSE, single-shot fast spin-echo.



**Table 4** Inter-reader agreement on inflammation in jejunum and ileum

Parameter	Image			
	DLR-NA	CR-NA	CR-A	DLR-A
Jejunum				
Mural thickness	0.656 (0.031–1.000)	0.656 (0.031–1.000)	0.656 (0.031–1.000)	0.656 (0.031–1.000)
Mural signal intensity	0.656 (0.031–1.000)	0.656 (0.031–1.000)	0.656 (0.031–1.000)	0.656 (0.031–1.000)
Perimural signal intensity	0.656 (0.031–1.000)	0.656 (0.031–1.000)	0.656 (0.031–1.000)	0.656 (0.031–1.000)
Ileum				
Mural thickness	0.621 (0.431–0.795)	0.621 (0.431–0.795)	0.588 (0.429–0.822)	0.588 (0.429–0.822)
Mural signal intensity	0.655 (0.485–0.831)	0.655 (0.485–0.831)	0.655 (0.521–0.855)	0.655 (0.521–0.855)
Perimural signal intensity	0.529 (0.286–0.697)	0.529 (0.286–0.697)	0.529 (0.286–0.697)	0.529 (0.286–0.697)

Values in parentheses are the 95% confidence intervals. DLR-NA, SSFSE with deep learning-based reconstruction without antiperistaltic agent; CR-NA, SSFSE with conventional reconstruction without antiperistaltic agent; CR-A, SSFSE with conventional reconstruction with antiperistaltic agent; DLR-A, SSFSE with deep learning-based reconstruction with an antiperistaltic agent; SSFSE, single-shot fast spin-echo.

=1.00). The inter-reader agreement demonstrated moderate to good agreement ( $\kappa = 0.53$ – $0.66$  for all comparisons). The detailed results are presented in *Tables 4, 5*.

### Diagnostic performance

The diagnostic performance for detecting active inflammation in the terminal ileum was evaluated in each image using endoscopic findings within one week as the reference standard. Endoscopic results were available for 29 patients (7 males, 22 females; mean age  $\pm$  standard deviation,  $30.9 \pm 9.3$  years, ranged 16–52 years), with 18 of them having active inflammation in the terminal ileum. The average interval between the endoscopy and MRE was  $2.9 \pm 2.53$  days (range, 0–7 days). The sensitivity, specificity, and accuracy of DLR-A were 94.42%, 81.83%, and 89.69%; and 83.33%, 90.91%, and 86.21% for Readers 1 and 2, respectively. The presence of active inflammation assessment did not vary among the four image sets; therefore, the diagnostic performance was the same for DLR-NA, CR-A, and CR-NA, as it was for DLR-A (*Figure 1*).

Among 45 patients, 2 showed active inflammation in the jejunum according to the reference standard. The sensitivity, specificity, and accuracy of DLR-A in the jejunal loop were 50%, 100%, and 97.8%; and 100%, 100%, and 100% for Readers 1 and 2, respectively. It should be noted that active inflammation was only observed in two cases of the jejunal loop, which may have contributed to the low sensitivity findings for Reader 1 (*Figures 2, 3*). The diagnostic performance for active inflammation in jejunum

was also the same among four image sets.

### SNR

At both the SMA and iliac bifurcation levels, DLR-A (mean values of  $117.15 \pm 24.19$  in the SMA level and  $120.80 \pm 18.42$  in the bifurcation) and DLR-NA ( $120.28 \pm 24.63$  in the SMA and  $123.05 \pm 23.98$  in the bifurcation) exhibited significantly higher SNR when compared to CR-NA ( $63.99 \pm 12.24$  in the SMA and  $61.46 \pm 12.35$  in the bifurcation) and CR-A ( $82.99 \pm 21.63$  in the SMA and  $80.38 \pm 19.77$  in the bifurcation). There were no significant differences between DLR-A and DLR-NA, but significant differences between CR-A and CR-NA in both the SMA and iliac bifurcation levels. The summarized results are in *Table 6*.

### Discussion

This study compared the image quality and diagnostic performance of four single breath-hold SSFSE image sets for patients with known Crohn's disease: namely conventional reconstruction with and without an anti-peristaltic agent, and deep learning-based reconstruction with and without an anti-peristaltic agent. When compared with DLR-A, DLR-NA demonstrated no significant difference in the overall image quality and artifacts, whereas DLR-A showed better image quality and fewer artifacts than both CR-A and CR-NA. Furthermore, DLR images showed significantly high SNR compared with CR images. The diagnostic performance for detecting

Table 5 Inter-image agreement on inflammation in the jejunum and ileum

Parameters	DLR-NA vs. CR-NA		DLR-NA vs. CR-A		DLR-NA vs. DLR-A		CR-NA vs. CR-A		CR-NA vs. DLR-A		CR-A vs. DLR-A	
	Reader 1	Reader 2	Reader 1	Reader 2	Reader 1	Reader 2	Reader 1	Reader 2	Reader 1	Reader 2	Reader 1	Reader 2
Jejunum												
Mural thickness	1.000 (1.000-1.000)	1.000 (1.000-1.000)	0.494 (0.483-0.505)	1.000 (1.000-1.000)	0.494 (0.483-0.505)	1.000 (1.000-1.000)	0.494 (0.483-0.505)	1.000 (1.000-1.000)	0.494 (0.483-0.505)	1.000 (1.000-1.000)	0.494 (0.483-0.505)	1.000 (1.000-1.000)
Mural signal intensity	1.000 (1.000-1.000)	1.000 (1.000-1.000)	1.000 (1.000-1.000)	1.000 (1.000-1.000)	1.000 (1.000-1.000)	1.000 (1.000-1.000)	1.000 (1.000-1.000)	1.000 (1.000-1.000)	1.000 (1.000-1.000)	1.000 (1.000-1.000)	1.000 (1.000-1.000)	1.000 (1.000-1.000)
Perimural signal intensity	1.000 (1.000-1.000)	1.000 (1.000-1.000)	1.000 (1.000-1.000)	1.000 (1.000-1.000)	1.000 (1.000-1.000)	1.000 (1.000-1.000)	1.000 (1.000-1.000)	1.000 (1.000-1.000)	1.000 (1.000-1.000)	1.000 (1.000-1.000)	1.000 (1.000-1.000)	1.000 (1.000-1.000)
Ileum												
Mural thickness	1.000 (1.000-1.000)	1.000 (1.000-1.000)	0.967 (0.906-1.000)	1.000 (1.000-1.000)	0.967 (0.906-1.000)	1.000 (1.000-1.000)	0.967 (0.906-1.000)	1.000 (1.000-1.000)	0.967 (0.906-1.000)	1.000 (1.000-1.000)	0.967 (0.906-1.000)	1.000 (1.000-1.000)
Mural signal intensity	1.000 (1.000-1.000)	1.000 (1.000-1.000)	0.967 (0.906-1.000)	1.000 (1.000-1.000)	0.967 (0.906-1.000)	1.000 (1.000-1.000)	0.967 (0.906-1.000)	1.000 (1.000-1.000)	0.967 (0.906-1.000)	1.000 (1.000-1.000)	0.967 (0.906-1.000)	1.000 (1.000-1.000)
Perimural signal intensity	1.000 (1.000-1.000)	1.000 (1.000-1.000)	1.000 (1.000-1.000)	1.000 (1.000-1.000)	1.000 (1.000-1.000)	1.000 (1.000-1.000)	1.000 (1.000-1.000)	1.000 (1.000-1.000)	1.000 (1.000-1.000)	1.000 (1.000-1.000)	1.000 (1.000-1.000)	1.000 (1.000-1.000)

Values in parentheses are the 95% confidence intervals. DLR-NA, SSFSE with deep learning-based reconstruction without antiperistaltic agent; CR-NA, SSFSE with conventional reconstruction without antiperistaltic agent; CR-A, SSFSE with conventional reconstruction with antiperistaltic agent; DLR-A, SSFSE with deep learning-based reconstruction with antiperistaltic agent; SSFSE, single-shot fast spin-echo.

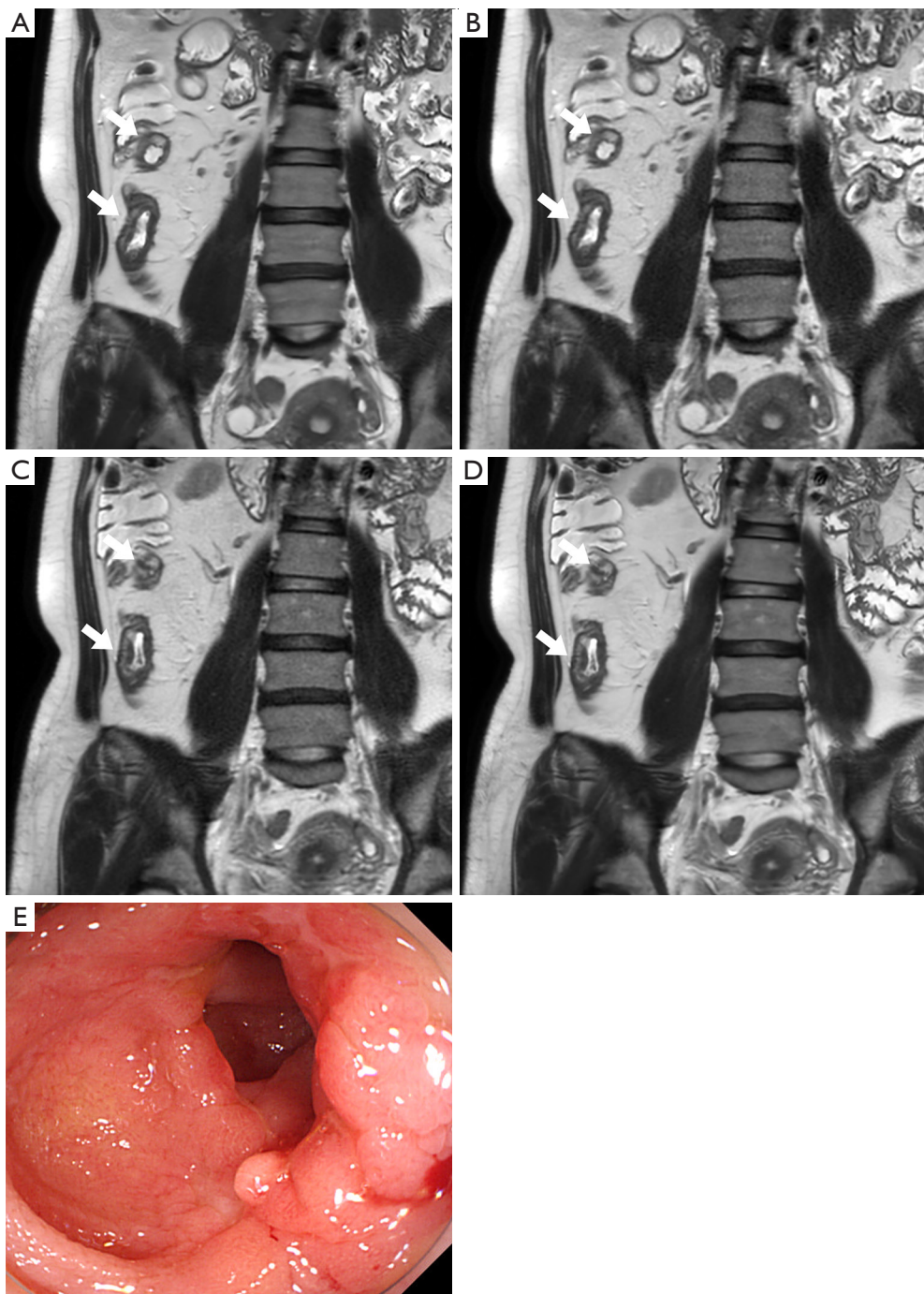


**Figure 1** Coronal SSFSE T2-weighted images of a 45-year-old patient with Crohn's disease. (A) DLR-NA, (B) CR-NA, (C) CR-A, (D) DLR-A, respectively. Wall thickening and increased mural signal intensity of terminal ileum and distal ileum (arrows) are noted in all images. Both readers gave identical scores in all four sequences regarding mural thickness, mural signal intensity, and perimural signal intensity. The endoscopy image of terminal ileum (E), performed 1 day after the MR enterography show erosions and ulcers with stenosis, corresponding to the inflammation in the terminal ileum noted in the images. SSFSE, single shot fast spin echo; DLR, deep learning-based reconstruction; CR, conventional reconstruction; NA, without anti-peristaltic agent; A, with anti-peristaltic agent; MR, magnetic resonance.



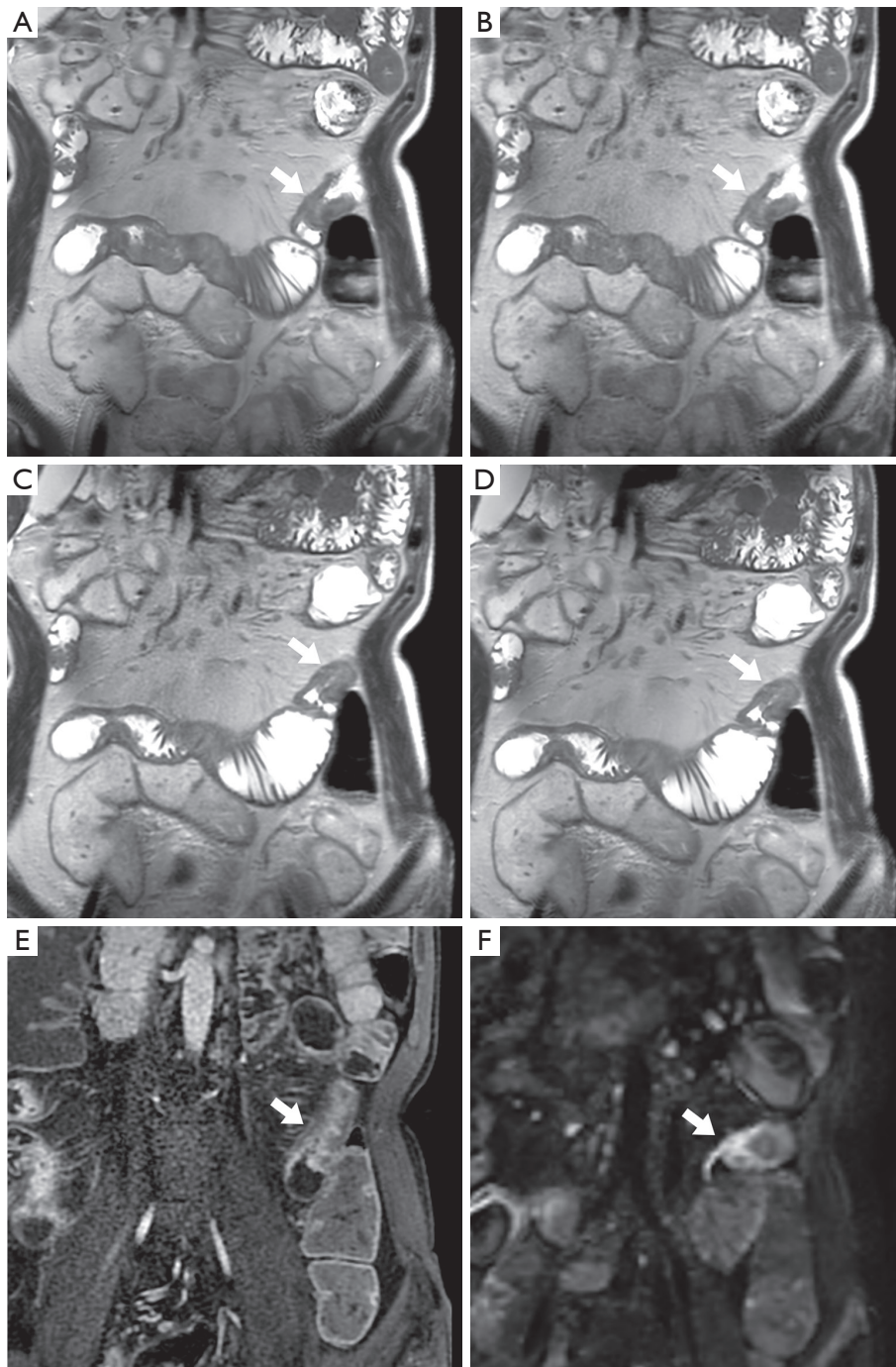


**Figure 2** Coronal SSFSE T2-weighted images of a 49-year-old patient with Crohn's disease. (A) DLR-NA, (B) CR-NA, (C) CR-A, (D) DLR-A, respectively. All images demonstrate wall thickening with increased T2 signal intensity in jejunum (arrows). Images without anti-peristaltic agents (A,B) show equivocal distension and visualization of the lesion compared to images with anti-peristaltic agent (B,C). Both readers gave identical scores in all four sequences regarding mural thickness, mural signal intensity, and perimural signal intensity. In arterial enhanced T1 weighted image (E), and diffusion weighted image ( $b = 900 \text{ s/m}^2$ ) (F), arterial enhancement and diffusion restriction, suggesting active inflammation. SSFSE, single shot fast spin echo; DLR, deep learning-based reconstruction; NA, without anti-peristaltic agent; CR, conventional reconstruction; A, with anti-peristaltic agent.

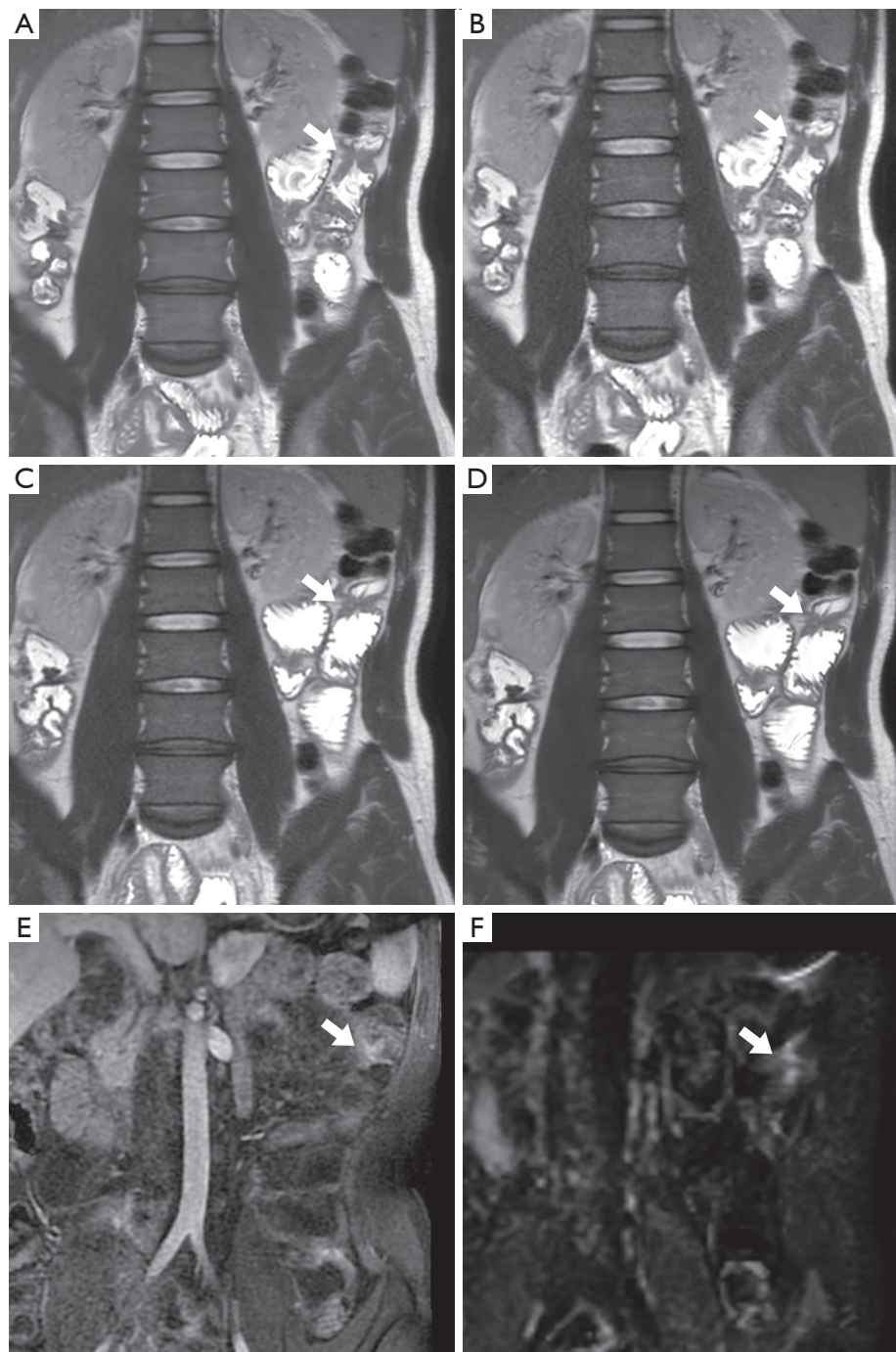


**Figure 3** Coronal SSFSE T2-weighted images of a 35-year-old patient with Crohn's disease. (A) DLR-NA, (B) CR-NA, (C) CR-A, (D) DLR-A, respectively. Focal wall thickening and increased mural signal intensity of jejunum (arrows) is noted in all images. The NA images (A,B) show slightly less distended jejunal lumen, but visualization of the lesion is not impaired. Reader 1 gave score 0 in mural thickness, mural signal intensity and perimural signal intensity in all four data sets, whereas Reader 2 gave 3, 2, 1 point, respectively. Possible cause of the discrepancy is that the lesion is relatively small in segment, with overall jejunum is not adequately distended in all four data sets. The arterial enhanced T1 weighted image (E) and diffusion weighted image ( $b = 900 \text{ s/m}^2$ ) (F) enhancement and diffusion restriction of the corresponding area, suggesting active inflammation. SSFSE, single shot fast spin echo; DLR, deep learning-based reconstruction; NA, without anti-peristaltic agent; CR, conventional reconstruction; A, with anti-peristaltic agent.

**Table 6** Comparison of signal-to-noise ratio in four images

SNR measured level	DLR-NA	DLR-A	CR-NA	CR-A
SMA level (mean $\pm$ SD)	120.28 $\pm$ 24.63	117.15 $\pm$ 24.19*	63.99 $\pm$ 12.24	82.99 $\pm$ 21.63
Bifurcation level (mean $\pm$ SD)	123.05 $\pm$ 23.98	120.80 $\pm$ 18.42*	61.46 $\pm$ 12.35	80.38 $\pm$ 19.77

\*, all comparison except for DLR-NA and DLR-A showed significant difference in signal-to-noise ratio in both SMA and bifurcation level ( $P < 0.001$ ). CR-A, SSFSE with conventional reconstruction with anti-peristaltic agent; CR-NA, SSFSE with conventional reconstruction without anti-peristaltic agent; DLR-NA, SSFSE with deep learning-based reconstruction without anti-peristaltic agent; DLR-A, SSFSE with deep learning-based reconstruction with an anti-peristaltic agent; SNR, Signal-to-noise ratio; SD, standard deviation; SMA, superior mesenteric artery; SSFSE, single-shot fast spin-echo.

active inflammation did not vary among the four image sets. Inter-reader and inter-image agreement of the parameters of active inflammation was fair to excellent. These results suggest that the effect of an anti-peristaltic agent on the image quality and artifacts of SSFSE in MRE is not as profound as that of DLR. Furthermore, the interpretation of parameters and diagnostic accuracy for active inflammation in Crohn's disease did not change with different reconstruction methods or with the omission of an anti-peristaltic agent.

Most studies on MRE have been conducted using MRE that incorporates anti-peristaltic agents. Although a few studies have reported the feasibility of performing MRE without an anti-peristaltic agent (2,20), the current guidelines recommend its use (3,4). Nevertheless, limited evidence exists on the effect of anti-peristaltic agents on the image quality of MRE or active inflammation diagnosis. In a previous study comparing MRE without anti-peristaltic agents to CT enterography (CTE), significant image degradation was observed in MRE without an anti-peristaltic agent; however, the diagnostic interpretation for the presence of active inflammation demonstrated substantial agreement with CTE (2). Another study examining the use of anti-peristaltic agents for DWI suggested that anti-peristaltic agents are necessary for DWI acquisition because omitting them could reduce the sensitivity of the diagnosis of active inflammation (8). This is the first study to investigate the effect of anti-peristaltic agents on the image quality and diagnostic performance of T2WI in MRE. Our results indicate that the omission of the use of anti-peristaltic agents did not affect the diagnosis of active inflammation upon T2WI of MRE.

DLR demonstrated improved image quality and reduced artifacts in SSFSE T2WI of abdominal MRI in previous studies (10,11). Our study further confirms the benefits of DLR in improving image quality and reducing artifacts

compared to CR. Furthermore, DLR revealed a more significant impact on image quality than the use of an anti-peristaltic agent for SSFSE of MRE. This is because SSFSE is relatively robust to motion, because each image is obtained within a single echo train; however, it possesses certain inherent limitations, such as reduced SNR owing to short acquisition time, blurring, and reduced image contrast due to T2 decay during the extended echo train (21). DLR can reduce these factors that cause image degradation. Additionally, peristaltic motility is decreased in the inflamed bowels of patients with Crohn's disease (22,23).

The protocols for the use of anti-peristaltic agents vary among institutions. Various anti-peristaltic agents are used, with glucagon being commonly used in the United States, and hyoscine butylbromide also is widely used. Additionally, hyoscine, hyoscyamine sulfate, cimetropium bromide, among others, can be used for anti-peristaltic effect (1). The administration route varies and includes intramuscular, intravenous routes, as well as sublingual administration. The majority of these medications have a rapid onset of action, typically within 1 to 2 min (24,25). Notably, the two most commonly utilized agents, glucagon and hyoscine butylbromide, have relatively short durations of effect (1,24). A previous study demonstrated that split-dose administration results in significantly decreased peristalsis compared with single-dose administration (5). Current guidelines recommend the administration of an anti-peristaltic agent as a split dose (4). At our institution, we administer anti-peristaltic agents as split doses at three different times: before T2WI, DWI, and contrast enhancement. Upon considering the results of our study, the administration of an anti-peristaltic agent before T2WI can be omitted, while preserving the image quality and diagnostic performance with the help of DLR. Although the omitted dose is small, it is important for making the examination more convenient with lower probability of side effects.



Regarding bowel distension, both the readers reported that the jejunum demonstrated significantly less distension in the images generated without the use of anti-peristaltic agents, and both readers found no difference in the ileal distension. Although significant difference was noted in both readers, the difference in the distension grade of the jejunum between image sets with and without anti-peristaltic agents was not large (without anti-peristalsis group: Reader 1,  $2.78 \pm 0.70$ ; Reader 2,  $2.73 \pm 0.72$ ; and with anti-peristalsis group: Reader 1,  $2.87 \pm 0.79$ ; Reader 2  $2.89 \pm 0.71$ ), suggesting that the jejunal loop distension is still insufficient even following the use of an anti-peristaltic agent. Fortunately, no significant clinical impact is observed concerning the diagnosis of active inflammation in Crohn's disease because the prevalence of CD in the jejunum is low (26,27). However, anti-peristaltic agents should be used in patients with suspected or previous history of inflammation in the jejunum.

Our study has certain limitations. First, it was a retrospective study. Second, some patients did not undergo ileocolonoscopy; therefore, they were excluded from the analysis of the diagnostic performance in the terminal ileum. Third, the readers could not be completely blinded to the image sets owing to the possibility of discerning the image sets according to different textures and distension of the bowel loops. Lastly, we scored image quality subjectively, but did not perform quantitative analyses such as measuring the SNR in this study. However, our very recent study demonstrated that DLR significantly increased the SNR of SSFSE T2WI in MR enterography (9).

## Conclusions

DLR improved the image quality and reduced artifacts in single breath-hold SSFSE T2-weighted MRE images more significantly than the use of an anti-peristaltic agent. Eliminating the use of an anti-peristaltic agent before SSFSE T2WI acquisition and adding DLR can be performed without affecting the image quality and diagnostic performance for active inflammation in patients with Crohn's disease. This result in a more convenient examination in terms of time and cost, with reducing the chance of exposure to potential side effects of anti-peristaltic agents.

## Acknowledgments

*Funding:* None.

## Footnote

*Conflicts of Interest:* All authors have completed the ICMJE uniform disclosure form (available at <https://qims.amegroups.com/article/view/10.21037/qims-23-738/coif>). J.L. is a current employee of GE HealthCare Korea, and his contribution was limited to assisting with statistical analysis. The other authors have no conflicts of interest to declare.

*Ethical Statement:* The authors are accountable for all aspects of the work in ensuring that questions related to the accuracy or integrity of any part of the work are appropriately investigated and resolved. The study was conducted in accordance with the Declaration of Helsinki (as revised in 2013). The study was approved by institutional review board of Inje University Haeundae Paik Hospital (No. HPIRB 2023-04-016-002) and individual consent for this retrospective analysis was waived.

*Open Access Statement:* This is an Open Access article distributed in accordance with the Creative Commons Attribution-NonCommercial-NoDerivs 4.0 International License (CC BY-NC-ND 4.0), which permits the non-commercial replication and distribution of the article with the strict proviso that no changes or edits are made and the original work is properly cited (including links to both the formal publication through the relevant DOI and the license). See: <https://creativecommons.org/licenses/by-nc-nd/4.0/>.

## References

1. Chatterji M, Fidler JL, Taylor SA, Anupindi SA, Yeh BM, Guglielmo FF. State of the Art MR Enterography Technique. *Top Magn Reson Imaging* 2021;30:3-11.
2. Grand DJ, Beland MD, Machan JT, Mayo-Smith WW. Detection of Crohn's disease: Comparison of CT and MR enterography without anti-peristaltic agents performed on the same day. *Eur J Radiol* 2012;81:1735-41.
3. Grand DJ, Guglielmo FF, Al-Hawary MM. MR enterography in Crohn's disease: current consensus on optimal imaging technique and future advances from the SAR Crohn's disease-focused panel. *Abdom Imaging* 2015;40:953-64.
4. Taylor SA, Avni F, Cronin CG, Hoeffel C, Kim SH, Laghi A, Napolitano M, Petit P, Rimola J, Tolan DJ, Torkzad MR, Zappa M, Bhatnagar G, Puylaert CAJ, Stoker J. The first joint ESGAR/ESPR consensus statement on the technical performance of cross-sectional small bowel and

- colonic imaging. *Eur Radiol* 2017;27:2570-82.
5. Rao A, Sitheequ F, Gustafson S, Lu M, Prior M. MR enterography - Impact on image quality between single-versus split-dose Buscopan. *J Med Imaging Radiat Oncol* 2020;64:331-7.
  6. Seo N, Park SH, Kim KJ, Kang BK, Lee Y, Yang SK, Ye BD, Park SH, Kim SY, Baek S, Han K, Ha HK. MR Enterography for the Evaluation of Small-Bowel Inflammation in Crohn Disease by Using Diffusion-weighted Imaging without Intravenous Contrast Material: A Prospective Noninferiority Study. *Radiology* 2016;278:762-72.
  7. Kim J, Seo N, Bae H, Kang EA, Kim E, Chung YE, Lim JS, Kim MJ. Comparison of Sensitivity Encoding (SENSE) and Compressed Sensing-SENSE for Contrast-Enhanced T1-Weighted Imaging in Patients With Crohn Disease Undergoing MR Enterography. *AJR Am J Roentgenol* 2022;218:678-86.
  8. Park SH, Huh J, Park SH, Lee SS, Kim AY, Yang SK. Diffusion-weighted MR enterography for evaluating Crohn's disease: Effect of anti-peristaltic agent on the diagnosis of bowel inflammation. *Eur Radiol* 2017;27:2554-62.
  9. Park EJ, Lee Y, Lee J. Impact of Deep-Learning Based Reconstruction on Single-Breath-Hold, Single-Shot Fast Spin-Echo in MR Enterography for Crohn's Disease. *J Korean Soc Radiol* 2023;84:e93.
  10. Lebel RM. Performance characterization of a novel deep learning-based MR image reconstruction pipeline. *arXiv preprint arXiv:200806559* 2020.
  11. Sheng RF, Zheng LY, Jin KP, Sun W, Liao S, Zeng MS, Dai YM. Single-breath-hold T2WI liver MRI with deep learning-based reconstruction: A clinical feasibility study in comparison to conventional multi-breath-hold T2WI liver MRI. *Magn Reson Imaging* 2021;81:75-81.
  12. Wang X, Ma J, Bhosale P, Ibarra Rovira JJ, Qayyum A, Sun J, Bayram E, Szklaruk J. Novel deep learning-based noise reduction technique for prostate magnetic resonance imaging. *Abdom Radiol (NY)* 2021;46:3378-86.
  13. Koch KM, Sherafati M, Arpinar VE, Bhave S, Ausman R, Nencka AS, Lebel RM, McKinnon G, Kaushik SS, Vierck D, Stetz MR, Fernando S, Mannem R. Analysis and Evaluation of a Deep Learning Reconstruction Approach with Denoising for Orthopedic MRI. *Radiol Artif Intell* 2021;3:e200278.
  14. Liu P, Wang Q, Peng C, Luo B, Zhang J. Combined application of isotropic three-dimensional fast spin echo (3D-FSE-Cube) with 2-point Dixon fat/water separation (FLEX) and 3D-FSE-cube in MR dacryocystography. *Br J Radiol* 2019;92:20180157.
  15. Hahn S, Yi J, Lee HJ, Lee Y, Lee J, Wang X, Fung M. Comparison of deep learning-based reconstruction of PROPELLER Shoulder MRI with conventional reconstruction. *Skeletal Radiol* 2023;52:1545-55.
  16. Lee SB, Kim SH, Son JH, Baik JY. Evaluation of bowel distension and bowel wall visualization according to patient positions during administration of oral contrast media for CT enterography. *Br J Radiol* 2017;90:20170352.
  17. Steward MJ, Punwani S, Proctor I, Adjei-Gyamfi Y, Chatterjee F, Bloom S, Novelli M, Halligan S, Rodriguez-Justo M, Taylor SA. Non-perforating small bowel Crohn's disease assessed by MRI enterography: derivation and histopathological validation of an MR-based activity index. *Eur J Radiol* 2012;81:2080-8.
  18. Pimpalkhute VA, Page R, Kothari A, Bhurchandi KM, Kamble VM. Digital Image Noise Estimation Using DWT Coefficients. *IEEE Trans Image Process* 2021;30:1962-72.
  19. Son JH, Lee Y, Lee HJ, Lee J, Kim H, Lebel MR. LAVA HyperSense and deep-learning reconstruction for near-isotropic (3D) enhanced magnetic resonance enterography in patients with Crohn's disease: utility in noise reduction and image quality improvement. *Diagn Interv Radiol* 2023;29:437-49.
  20. Grand DJ, Kampalath V, Harris A, Patel A, Resnick MB, Machan J, Beland M, Chen WT, Shah SA. MR enterography correlates highly with colonoscopy and histology for both distal ileal and colonic Crohn's disease in 310 patients. *Eur J Radiol* 2012;81:e763-9.
  21. Bhosale P, Ma J, Choi H. Utility of the FIESTA pulse sequence in body oncologic imaging: review. *AJR Am J Roentgenol* 2009;192:S83-93 (Quiz S94-7).
  22. Bickelhaupt S, Pazahr S, Chuck N, Blume I, Froehlich JM, Cattin R, Raible S, Bouquet H, Bill U, Rogler G, Frei P, Boss A, Patak MA. Crohn's disease: small bowel motility impairment correlates with inflammatory-related markers C-reactive protein and calprotectin. *Neurogastroenterol Motil* 2013;25:467-73.
  23. Bickelhaupt S, Froehlich JM, Cattin R, Patuto N, Tutuian R, Wentz KU, Culmann JL, Raible S, Bouquet H, Bill U, Patak MA. Differentiation between active and chronic Crohn's disease using MRI small-bowel motility examinations - initial experience. *Clin Radiol* 2013;68:1247-53.
  24. Froehlich JM, Daenzer M, von Weyarn C, Erturk SM, Zollikofer CL, Patak MA. Aperistaltic effect of hyoscine N-butylbromide versus glucagon on the small bowel



- assessed by magnetic resonance imaging. *Eur Radiol* 2009;19:1387-93.
25. Dillman JR, Smith EA, Khalatbari S, Strouse PJ. I.v. glucagon use in pediatric MR enterography: effect on image quality, length of examination, and patient tolerance. *AJR Am J Roentgenol* 2013;201:185-9.
26. Torres J, Mehandru S, Colombel JF, Peyrin-Biroulet L. Crohn's disease. *Lancet* 2017;389:1741-55.
27. Ng SC, Tang W, Ching JY, Wong M, Chow CM, Hui AJ, et al. Incidence and phenotype of inflammatory bowel disease based on results from the Asia-pacific Crohn's and colitis epidemiology study. *Gastroenterology* 2013;145:158-165.e2.

**Cite this article as:** Park EJ, Lee Y, Lee HJ, Son JH, Yi J, Hahn S, Lee J. Impact of deep learning-based reconstruction and anti-peristaltic agent on the image quality and diagnostic performance of magnetic resonance enterography comparing single breath-hold single-shot fast spin echo with and without anti-peristaltic agent. *Quant Imaging Med Surg* 2024;14(1):722-735. doi: 10.21037/qims-23-738

**Table S1** Imaging scan parameters

Parameters	Coronal SSFSE T2-weighted images without fat saturation
Refocusing flip angles (degree)	Initial 155°, 130°
Bandwidth (Hz/pixel)	90.91
Matrix	400×320
FOV	380×380
No. of slice acquired	36
Slice thickness (mm)	4
Slice gap (mm)	0.4
Acceleration factor	2.00
Reconstruction method for conventional reconstruction	Autocalibrating reconstruction for Cartesian imaging (ARC)
NEX	1.0
Echo time (ms)	80
Repetition time (ms)	1,287.9
Scan time (s), mean ± SD	53.19±3.16

SSFSE, single shot fast spin echo; FOV, field of view; SD, standard deviation.